Carbon Letters (2022) 32:181–191
https://doi.org/10.1007/s42823-021-00265-y

Online ISSN 2233-4998
Print ISSN 1976-4251

ORIGINAL ARTICLE

Ultra-trace detection of toxic heavy metal ions using graphitic carbon functionalized Co_3O_4 modified screen-printed electrode

R. T. Yogeeshwari[1,2] · R. Hari Krishna[1] · Prashanth S. Adarakatti[3] · S. Ashoka[4]

Received: 4 March 2021 / Revised: 13 June 2021 / Accepted: 28 June 2021 / Published online: 6 July 2021

Abstract

Herein, a new and generic strategy has been proposed to introduce uniformly distributed graphitic carbon into the nanostructured metal oxide. A facile and generic synthetic protocol has been proposed to introduce uniformly distributed conducting graphitic carbon into the Co_3O_4 nanoparticles (Co_3O_4 NPs@graphitic carbon). The prepared Co_3O_4 NPs@graphitic carbon has been drop casted onto the portable screen-printed electrode (SPE) to realize its potential application in the individual and simultaneous quantification of toxic Pb(II) and Cd(II) ions present in aqueous solution. The proposed Co_3O_4 NPs@graphitic carbon-based electrochemical sensor exhibits a wide linear range from 0 to 120 ppb with limit of detection of 3.2 and 3.5 ppb towards the simultaneous detection of Pb(II) and Cd(II), which falls well below threshold limit prescribed by WHO.

Keywords Co_3O_4 · Graphitic carbon · Screen-printed electrode · Pb(II) and Cd(II)

1 Introduction

In recent years, a serious concern about the heavy metal ions contamination even at trace-level results an adverse effect on human and aquatic life owing to their non-biodegradable characteristics and extreme toxicity. Particularly, the long term exposure of living organisms to Cd(II) can adversely affect the functioning of kidney and liver [1]. Similarly, exposure to Pb(II) could result diseases related to neurological, immunological and cardiovascular [2, 3]. Therefore, the fabrication of reliable and portable sensors to monitor heavy metal ions has gained significant research interest in recent years. Electrochemical detection and quantification of heavy metal ions offer potential advantages owing to their high sensitivity/selectivity, simple operation and capable of determining multiple ions simultaneously. Carbon paste electrode and glassy carbon electrode were extensively used in the fabrication of electrochemical sensors [4–6]. However, these electrodes are not suitable for on-field applications. To address this, electrochemical sensors based on screen-printed electrode (SPE) were considered as miniaturized electrode and potentially suitable for on-field detection of toxic heavy metal ions. These SPE's can be produced cheaply on large scale production and can be used as single-shot disposable electrodes. However, SPE's require suitable modifiers to achieve enhanced performance in terms of selectivity, sensitivity and limit of detection. In similar lines, numerous modifiers including metal and non-metal based materials were reported in the literature. For instance, single-walled carbon nanohorns [7], microporous Mn_2O_3 [8], bismuth nanoparticle-porous carbon nanocomposite [9], ionic liquid/carbon nanofibers/bismuth particles [10], polyoxometalate-based crystalline materials [11], Fe_3O_4@CNC/Cu [12] were proposed to modify the SPE for the detection of heavy metal ions. Among these oxide based nanostructured materials were considered as superior modifiers owing to their outstanding electro-catalytic activity. However, the poor or lower electronic conductivity of oxide based materials hinders their potential applications since it significantly affects the sensing performance (sensitivity and detection limit). Recently, nano-engineering, addition of dopants and conducting carbon-based materials has been widely adopted

✉ R. Hari Krishna
rhk.chem@gmail.com

[1] Department of Chemistry, M. S. Ramaiah Institute of Technology, Affiliated to Visvesvaraya Technological University, Bengaluru 560054, India

[2] Department of Chemistry, Seshadripuram College, Bengaluru 560068, India

[3] Department of Chemistry, SVM Arts, Science and Commerce College, Ilkal 587125, India

[4] Department of Chemistry, School of Engineering, Dayananda Sagar University, Bengaluru 560068, India

to enhance the electronic conductivity [13–15]. However, a new robust and generic strategy is essential to overcome the conductivity problem associated with the oxide based materials. Introducing conducting graphitic carbon during the preparation of metal oxide enables uniform distribution, which significantly enhances the conductivity and thereby electrochemical performance as well. Particularly, graphitic carbon has been introduced into the Co_3O_4 nanoparticles wherein the aqueous solution of cobalt nitrate hexahydrate and citric acid was subjected for thermal treatment at 500 °C for short time of 4 min. The in situ addition of conducting graphitic carbon in to the Co_3O_4 in short time, uniform distribution of Co_3O_4 nanoparticles is significant advancement in sensor technology to enhance the sensing performance. The prepared Co_3O_4 NPs@graphitic carbon has been used to modify the SPE. Then, the Co_3O_4 NPs@graphitic carbon modified SPE is used for the detection and quantification of Pb(II) and Cd(II) ions present in aqueous solution, individually and simultaneously.

2 Experimental

2.1 Preparation of electrocatalyst

The preparation of Co_3O_4@graphitic carbon nanoparticles was carried out according to our recently reported synthesis protocol [16]. The schematic representation of the preparation of graphitic carbon functionalized Co_3O_4 is shown in Fig. 1. Briefly, 1.71 mmol of cobalt nitrate hexahydrate and 9.517 mmol of anhydrous citric acid were dissolved in 7 mL of water containing 100 mL glass beaker. The resulting pink colored solution is subjected for thermal treatment at 500 °C for 4 min where it undergoes controlled and smoldering type combustion, which gives uniformly distributed Co_3O_4 on graphitic carbon nanoparticles. Then, the resulting black colored powder was crushed and used for further studies. In the process of synthesis, combustion time plays an important role in controlling the retention of the graphitic carbon and is optimized to 4 min.

2.2 Fabrication of Co_3O_4 nanoparticles@graphitic carbon modified SPE

5 mg of the as-prepared Co_3O_4 NPs@graphitic carbon was mixed with 5 mL of deionized water through sonication to prepare ink. Subsequently, 5 µL of the prepared ink was casted on the wording area of the screen-printed electrode and dried under infra-red lamp for ~ 30 min. The resulting Co_3O_4 NPs@graphitic carbon modified SPE has been used for the quantification of Pb(II) and Cd(II) ions.

2.3 Electrocatalyst characterization

The crystal structure and phase formation of the prepared Co_3O_4 NPs@graphitic carbon was studied using X-ray diffractometer (PANalytical X'pert PRO). The presence of graphitic carbon in the prepared Co_3O_4 is identified using Fourier transform infra-red spectrophotometer (ASB1716801/i55 Thermo Fisher scientific) and Raman spectrophotometer (Jobin Yvon LabRam HR). The microstructure and particle size of the Co_3O_4 NPs@graphitic carbon were investigated using transmission electron microscopy (Hitachi H-7500). Thermal gravimetric analysis (TGA) of the sample was carried out on a Shimadzu TA-50 thermal analyzer at a heating rate of 10 °C/min.

2.4 Electrochemical performance measurements

Electrochemical measurements toward the quantification of Pb(II) and Cd(II) ions, at room temperature, was performed using Biologic SP 150 electrochemical work station. The working, reference and counter electrode were made of Co_3O_4 NPs@graphitic carbon, Ag|AgCl and platinum electrode, respectively. Electrochemical performance of Co_3O_4 NPs@graphitic carbon modified SPE towards the detection of Pb(II) and Cd(II) ions were measured in acetate buffer, between the potential − 1.1 and 0 V *vs* Ag/AgCl using CV and differential pulse anodic stripping voltammetry (DPASV) techniques.

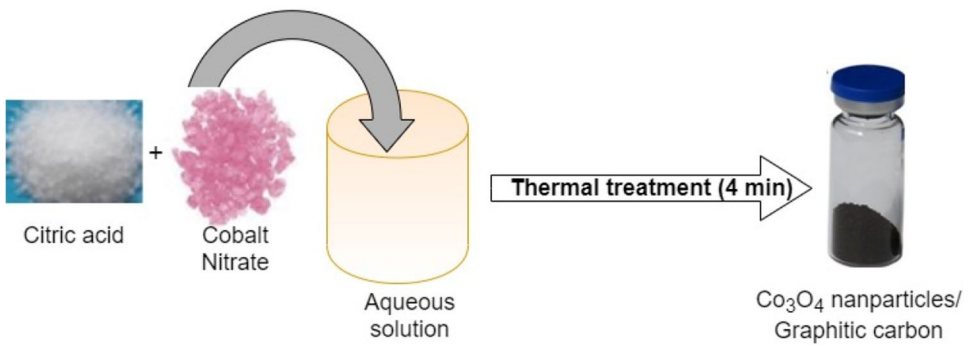

Fig. 1 Schematic representation of the preparation of Co_3O_4 nanoparticles@graphitic carbon nanoparticles

Known amount of analytes (Pb(II) and Cd(II) ions) and acetate buffer solution of pH 5 (8 mL) and supporting electrolyte KCl (2 mL) were taken in an electrochemical cell. Then, the Co_3O_4 nanoparticles@graphitic carbon modified SPE was immersed in the electrochemical cell. Analytes were pre-concentrated on the electrode surface by stirring for about one minute at open circuit. The pre-concentrated analytes were reduced at a reduction potential of − 0.5 V followed by stripped off from the Co_3O_4 NPs@graphitic carbon modified SPE into the bulk of the electrolytic solution. The observed anodic current was measured against applied potential.

3 Results and discussion

3.1 Structural and morphological studies

Aqueous solution of citric acid fuel and cobalt nitrate was subjected for thermal treatment at 500 ℃, which results in formation of thick gel and then the formed thick gel undergoes controlled combustion to get a pure metal oxide in nano regime. The formation of nanostructured Co_3O_4 is represented according to the following reaction [17].

$$27Co(NO_3)_2 + 14C_6H_2O \rightarrow 9Co_3O_4 + 84CO_2 + 27\,N_2 + 56H_2O$$

The as-prepared Co_3O_4 NPs@graphitic carbon is systematically characterized using XRD, FTIR and Raman spectrum. The powder XRD pattern of the graphitic carbon functionalized Co_3O_4 is presented in Fig. 1a. The diffraction peaks appeared in the XRD pattern clearly demonstrates the formation of pure Co_3O_4 phase where the characteristic diffraction peaks appeared at 30.77°, 36.27°, 38.16°, 44.35°, 55.18°, 58.96° and 64.98° corresponds to (220), (311), (222), (400), (422), (511) and (440) crystalline planes of cubic Co_3O_4 [JCPDS 74 1657]. The presence of graphitic carbon is confirmed by the presence of sp^3 hybridized D and sp^2 hybridized G band in FTIR and Raman spectrum [16]. The HRTEM image, presented in Fig. 2d, indicates the uniform distribution of Co_3O_4 nanoparticles in graphitic

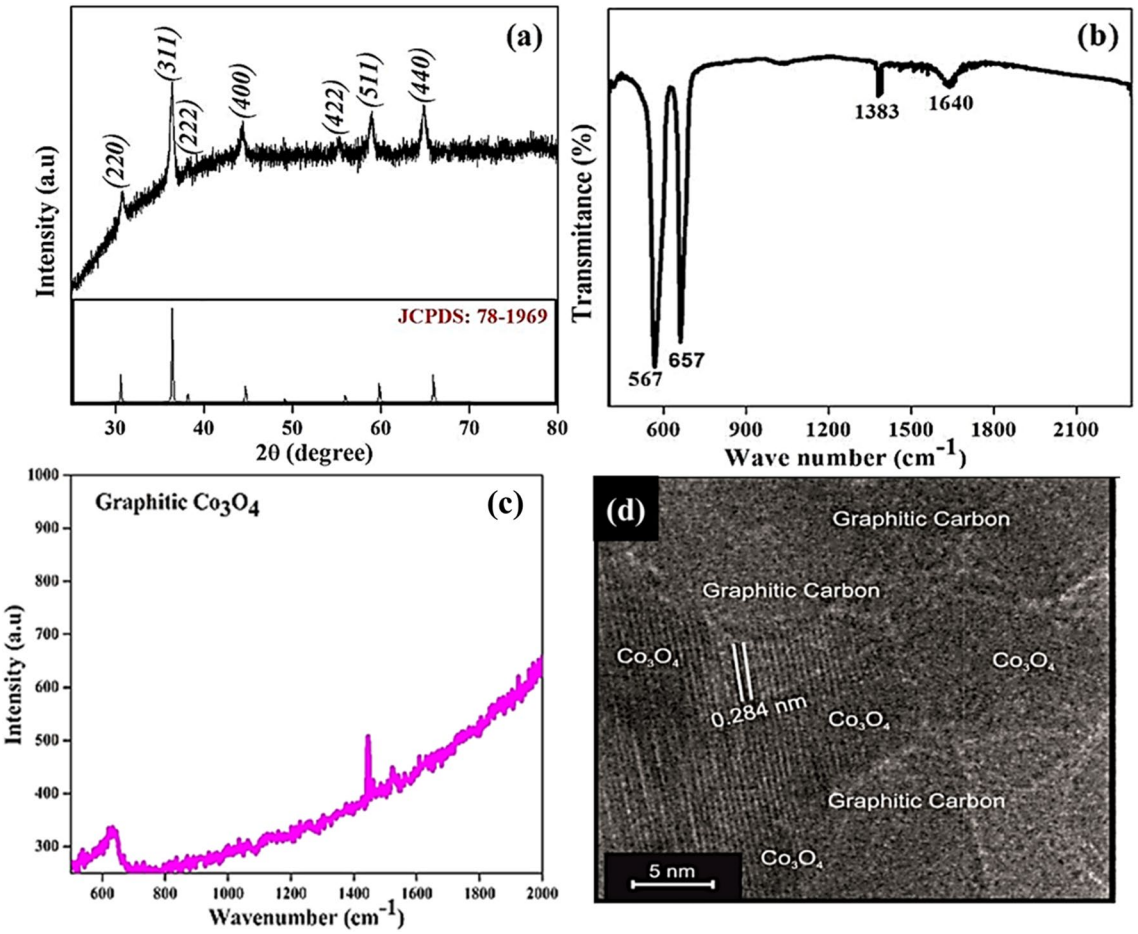

Fig. 2 **a** Powder XRD pattern, **b** FTIR spectrum, **c** Raman spectrum and **d** HRTEM image of Co_3O_4 NPs@graphitic carbon

carbon. Further, inter planar distance spacing of 0.284 nm corresponds to (220) plane of Co_3O_4. It is worth note that the proposed method not only retains the conducting graphitic carbon but also ensures the uniform distribution of graphitic carbon and thereby significantly enhances the charge transfer rate, which is important parameter in enhancing the performance of the electrochemical sensor. The content of graphitic carbon is controlled by controlling the combustion time. The as-prepared Co_3O_4 NPs@graphitic carbon was analyzed using TGA (figure not shown) to know quantity of graphitic carbon where the weight ratio of Co_3O_4 and graphitic carbon is found to be ~94:6.

3.2 Electrochemical impedance spectroscopy

Electrochemical impedance spectroscopic measurements were carried out in 5 mM ferricyanide solution between the frequency 0.1 mHz and 100 K Hz to exploit the information regarding the impedance difference between bare and modified SPE. The Nyquist plot of both bare and Co_3O_4 NPs@graphitic carbon modified SPE, presented in Fig. 3, consist of semicircle demonstrate the charge transfer resistance (Rct). Further, linear sloping line indicates the diffusion process. The bare SPE exhibits the Rct value of 11,200 Ω while Co_3O_4@graphitic carbon modified SPE exhibits the decreased Rct value of 6800 Ω. This impulsive decrease in the charge transfer resistance for Co_3O_4 NPs@graphitic carbon modified SPE reveals the more conductive nature and faster electron transfer rate as compared to the bare SPE. It is evident from the impedance results that the improved electrochemical performance is due to the synergetic effect of Co_3O_4 nanoparticle geometry and graphitic carbon. The presence of graphitic carbon ensures the uniform distribution of Co_3O_4 nanoparticles in graphitic carbon matrix and due to its conducting nature significantly enhances the charge transfer rate, which is important parameter in enhancing the performance of the electrochemical sensor.

3.3 Cyclic voltammetry study

The preliminary studies on electrochemical sensing of Co_3O_4 NPs@graphitic carbon modified SPE was carried out in presence of 10 mM of Pb(II) and Cd(II) ions, acetate buffer of pH 5 and 0.1 M KCl as supporting electrolyte at scan rate of 10 mV/s, using cyclic voltammetry (CV). Figure 4 presents the CV signatures of bare and Co_3O_4 NPs@graphitic carbon modified SPE with and without Pb(II) and Cd(II) analytes. As shown in the Fig. 4, no analytical signal (oxidation peak) observed for the bare SPE in the absence of the Pb(II) and Cd(II) metal ions while the same electrode shows a moderate response in the presence of Pb(II) and Cd(II) ions at − 0.65 V and − 0.85 V respectively. Further, the Co_3O_4 NPs@graphitic carbon modified SPE does not show any CV response towards Pb(II) and Cd(II). However, the enhanced analytical response with neat redox peaks appeared at − 0.65 V and − 0.85 V for Co_3O_4 NPs@graphitic carbon modified SPE in presence of Pb(II) and Cd(II) ions. The observed peak potential of − 0.65 V and − 0.85 V for Pb(II) and Cd(II) are in good agreement with the previous reports [18]. The enhanced response towards Pb(II) and Cd(II) is due to the more conductive nature and faster electron transfer rate of Co_3O_4 NPs@graphitic carbon modified SPE. Therefore, the Co_3O_4 NPs@graphitic carbon modified SPE could be used for the selective and sensitive detection of Pb(II) and Cd(II) ions in real sample matrices.

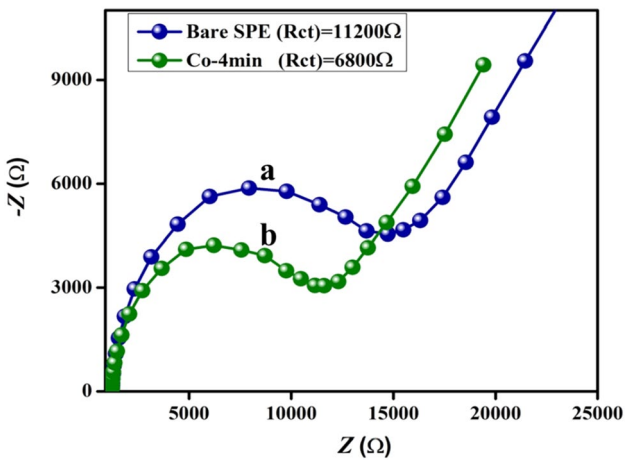

Fig. 3 Electrochemical impedance spectra of **a** bare and **b** Co_3O_4 NPs@graphitic carbon modified SPE in 5 mM potassium ferricyanide solution

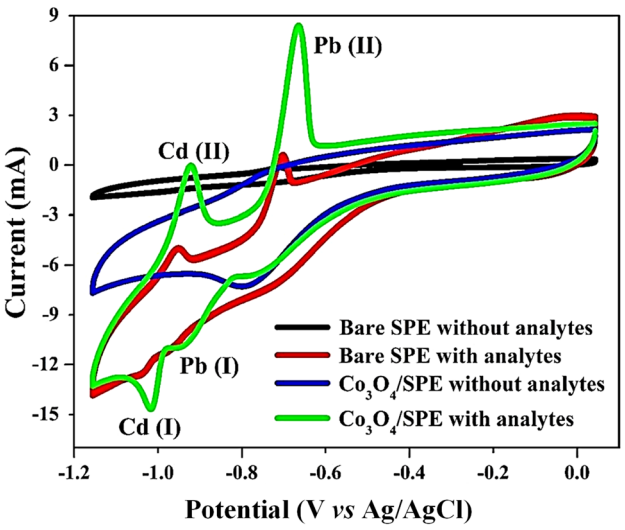

Fig. 4 CV at Co_3O_4@graphitic carbon modified SPE in the presence of Cd(II) and Pb(II) ions (10 mM) in acetate buffer solution of pH 5 at a scan rate of 10 mV/s

3.4 Optimization study

Generally, experimental variables like pH, deposition time and reduction potential significantly affect the sensing performance. Therefore, these variables have been optimized using differential pulse anodic stripping voltammetry (DPASV) to achieve the maximum sensing efficiency of the proposed Co_3O_4 NPs@graphitic carbon modified SPE towards Pb(II) and Cd(II) ions.

3.5 Effect of pH

The effect of pH was examined in presence of 100 ppb of Pb(II) and Cd(II) ions individually. Figure 5(a, b) illustrates the anodic peak current response of Pb(II) at different pH values of 3, 4, 5 and 6. The anodic peak current increases with increase in pH from 3 to 5 and then decreases at pH 6. Similarly, the Cd(II) also exhibits maximum anodic peak current at pH value of 5 (Fig. 5c,d). The increase in anodic peak current from pH of 3 to 5 and decreasing anodic peak current after pH 6 is explained as follows. At sufficiently low pH, the Pb(II) and Cd(II) ions has to compete with hydrogen ion for adsorption site on the working electrode surface. While, as the pH increases, the competition weakens and thereby more Cd(II) and Pb(II) ions adsorb on the electrode surface, which enhances the anodic current by participating in redox reaction. However, further increase in pH leads to the formation of hydroxide of Pb(II)/Cd(II) precipitate and thus anodic peak current decreases [19–21]. Hence, pH value of 5 is considered as optimum for further optimization studies.

3.6 Effect of deposition potential

Figure 6 presents the effect of deposition potential on the anodic peak current of Pb(II) and Cd(II). The anodic peak current increases up to − 0.5 V while decreases thereafter for both Pb(II) and Cd(II) ions. The increase of peak current is due to increase in extent of reduction of more and more Pb(II) and Cd(II) ions. Whereas, the decrease in

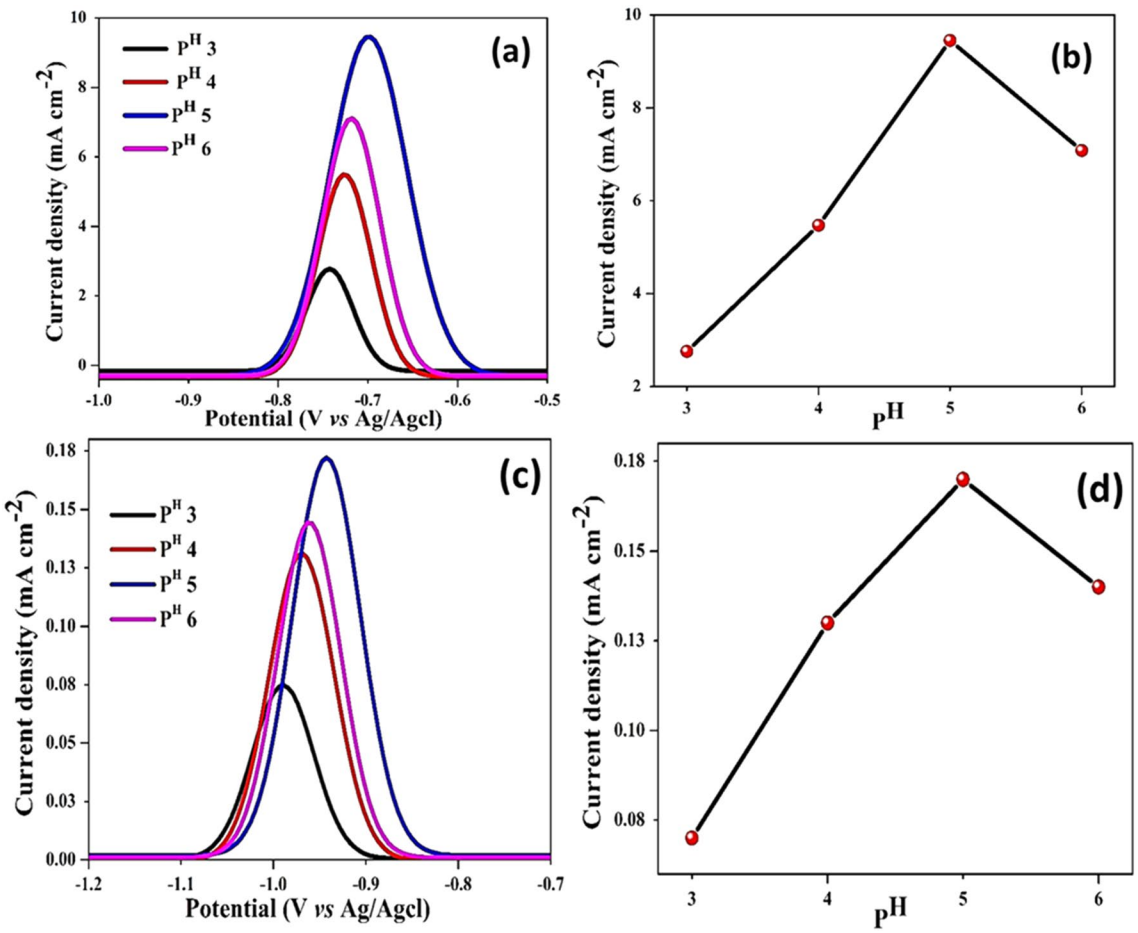

Fig. 5 Effect of pH on the stripping peak currents of 100 ppb Pb(II) and Cd(II): **a** overlaid DPV of Pb(II) ions, **b** plot of peak current and **c** overlaid DPV of Cd(II) ions and **d** plot of peak current

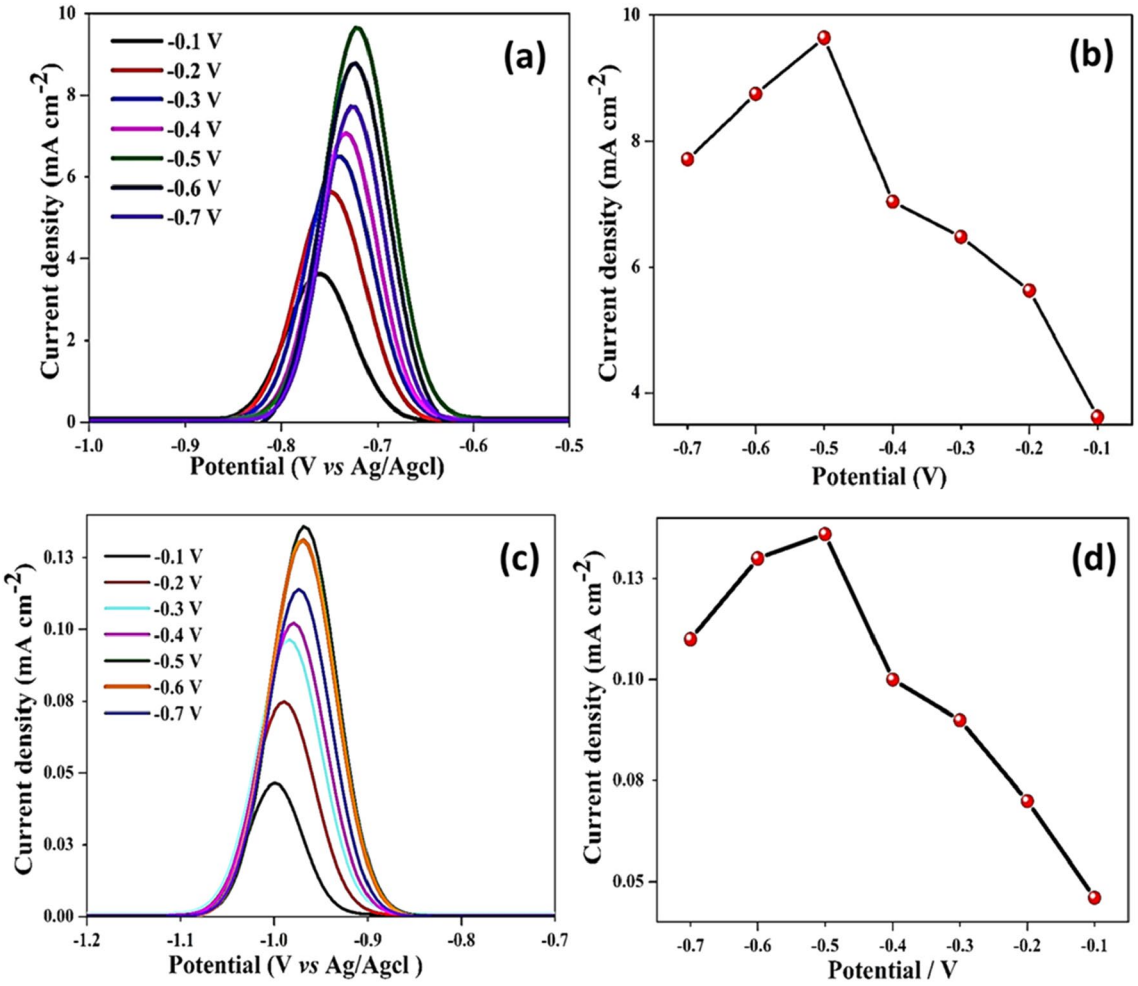

Fig. 6 Effect of deposition potential on the stripping peak currents; **a** overlaid DPV of Pb(II) ions, **b** plot of peak current and **c** overlaid DPV of Cd(II) ions and **d** plot of peak current

peak current at higher deposition potential is may be due to the formation of inter-metallic compounds [22–25]. Therefore, reduction potential of − 0.5 V was considered as an optimum reduction potential.

3.7 Effect of deposition time

Figure 7 presents the optimization of pre-concentration time for Pb(II) and Cd(II) ions. As shown in the Fig. 7, the anodic peak current of both Pb(II) and Cd(II) ions increases with increase in pre-concentration time, up 120 s. The increase of peak current is due to the fact that longer pre-concentration time results in the accumulation of more and more Pb(II) and Cd(II) on the electrode/solution interface. Hence deposition time of 120 s is considered as optimized time.

3.8 Individual determination of Pb(II) and Cd(II)

A calibration plot has been constructed, for the quantification of Pb(II) and Cd(II) ions individually, under optimized experimental conditions of pH 5, reduction potential − 0.5 V and deposition time 120 s. The observed results were summarized in Fig. 8 where the peak current of both Pb(II) and Cd(II) increases proportionately with increase of concentration. The current response of both Pb(II) and Cd(II) ions exhibit linearity with concentration range 0–120 ppb for Pb(II) and 0–90 ppb for Cd(II). The linear equation for Pb(II) and Cd(II) is found to be i/mA = 0.8957 + 0.07486 X and i/mA = 1.339 + 0.163 X, respectively. The limit of detection was calculated, based on the 3 sigma method, was found to be 3.2 nM for Pb(II) and 3.5 nM for Cd(II). The observed limit of detection is well within the threshold limits prescribed by WHO [26], demonstrating that the Co_3O_4

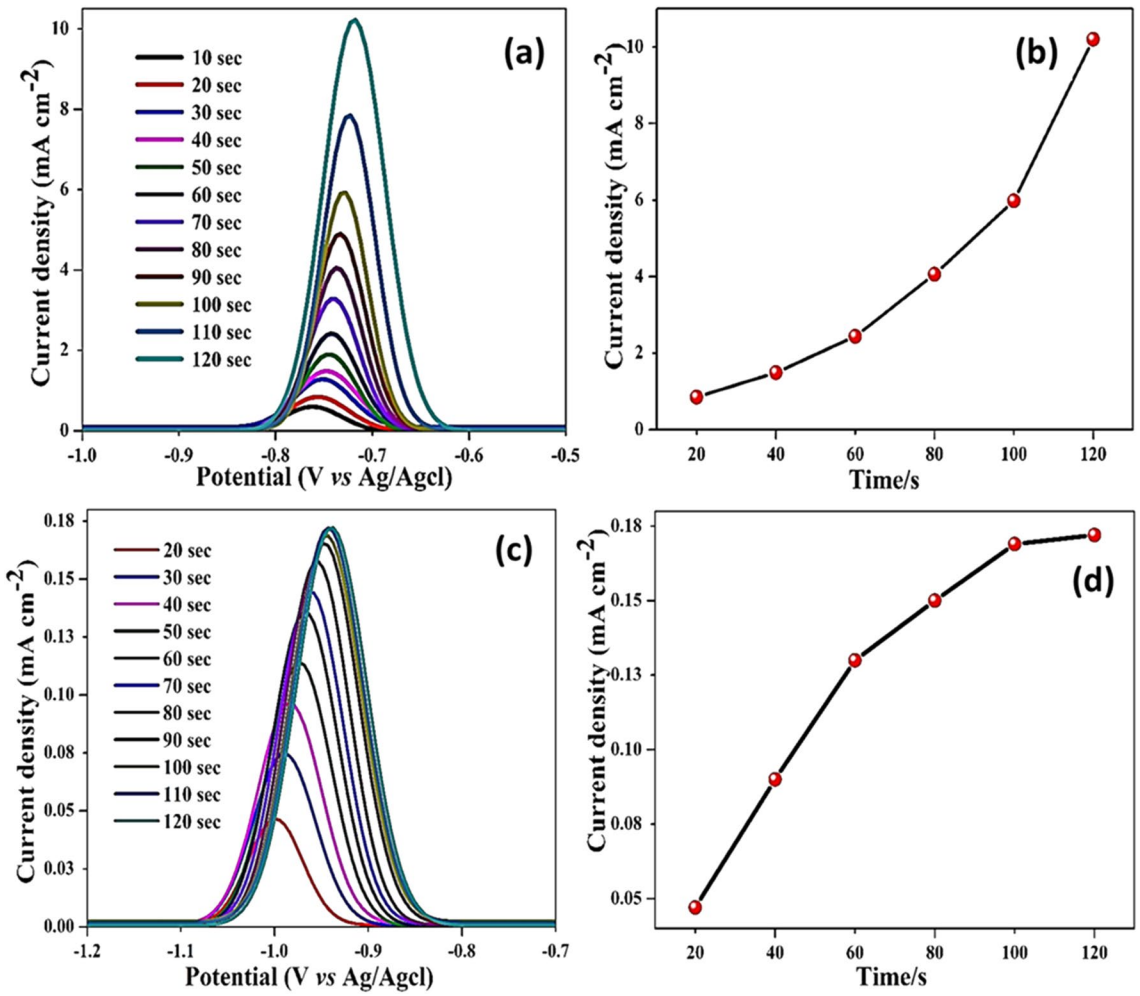

Fig. 7 Effect of pre-concentration time on the stripping currents; **a** overlaid DPV of Pb(II) ions, **b** plot of peak current and **c** overlaid DPV of Cd(II) ions and **d** plot of peak current

NPs@graphitic carbon modified SPE is highly sensitive even at very low concentration of Pb(II) and Cd(II) ions.

3.9 Simultaneous determination of Pb(II) and Cd(II)

The modified SPE has been successfully applied for the simultaneous measurement of Pb(II) and Cd(II) ions under optimal experimental conditions and the typical response DPASV was presented in Fig. 9. Further, the mixtures containing 10–120 ppb of each of the two metal ions were tested and it shows two anodic peaks at − 0.85 and − 0.65 V ascribed to Cd(II) and Pb(II) respectively (Fig. 9a). Further, the clear peak separation in the voltammetric peaks is large enough to quantify Pb(II) and Cd(II) separately. As shown in the Fig. 9(b, c), the linearization equation for Pb(II) and Cd(II) is found to be i/mA = 4.1429 + 0.1921c/ppb (correlation coefficients of 0.969) and i/mA = 0.3979 + 0.0903c/ppb (correlation coefficients of 0.987). The limit of detection (for Pb(II) and Cd(II) was determined, based on 3σ method, is found to be 3.2 and 3.5 ppb respectively. Hence, the simultaneous determination of the Pb(II) and Cd(II) ions could be determined using the proposed Co_3O_4 NPs@graphitic carbon /SPE sensor in 2 min.

The observed linear range and detection limit of the proposed Co_3O_4 NPs@graphitic carbon /SPE sensor has been compared with the selected electrochemical sensors, presented in Table 1, where it exhibits comparatively better linear range and detection limit.

3.10 Stability and repeatability of the proposed sensor

The simultaneous measurements of Pb(II) and Cd(II) at Co_3O_4 NPs@graphitic carbon /SPE in presence 100 ppb each of these ions were examined. The proposed Co_3O_4 NPs@graphitic carbon /SPE possess good stability, retaining their performance characteristics over a period of 2 months. The life span of the modified electrode was around 2 months

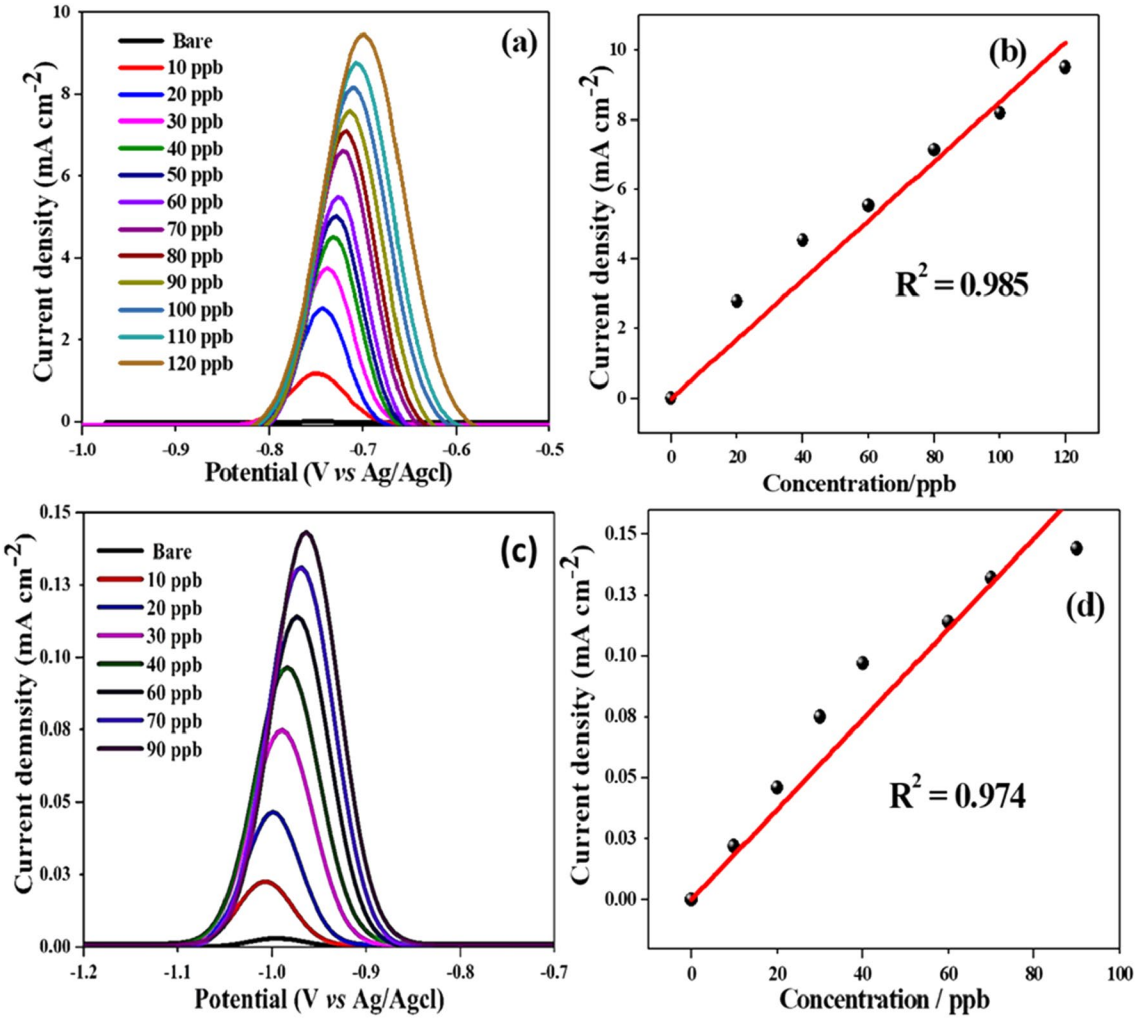

Fig. 8 Overlaid stripping voltammograms at different concentrations of Pb(II) and Cd(II) under optimized measurement (**a**–**c**). The corresponding calibration plots are shown (**c**, **d**)

(15 determinations). The Co_3O_4 NPs@graphitic carbon/SPE exhibited good repeatability, with relative standard deviations of 3.15% and 4.21% for Pb(II) and Cd(II) ions, respectively, for five successive runs. These experimental results revealed that the proposed sensor can be used over a period of time and continuous analysis with precise analytical measurements. Hence, it can be used for the measurements of target metal ions at trace-level concentration [27].

3.11 Interference study

The presence of interfering ions significantly affects the selectivity and sensitivity towards sensing of target metal ions and therefore the proposed Co_3O_4 NPs@graphitic carbon /SPE has been examined in presence of selected cations and anions, which generally coexist in many real sample matrices. The possible mutual interferent species were added into the electrolytic solution containing target analytes of 100 ppb of Pb(II) and Cd(II) and their impacts on the anodic peak currents were explored. Most of the cations and anions did not affect the simultaneous detection of Pb(II) and Cd(II) ions, when the optimized procedure was applied. The concentration of 500 fold of Cl^-, F^-, SO_4^{2-}, K^+, Mn(II), Li^+, Ag^+; 100 fold for Co(II), $C_2O_4^{2-}$ and CO_3^{2-}; 20 fold for As(III), Cr(VI), and F^-; tenfold of Ni(II) and Fe(II) were tested. The observed results indicate the signal deviations of 100 ppb of Pb(II) and Cd(II) are not larger than 5%. Further, the ions such as Zn(II), Hg(II), and Cu(II) have shown severe interference on the stripping current response of Pb(II) and Cd(II) ions. Experimental results show that Zn(II) and Hg(II) (fivefold excess) do not interfere significantly. However, Cu(II) (two-fold excess) significantly decreased the peak intensity, nearly up to 50%. The decrease in the peak current may be due to the formation of an inter-metallic compound between copper and Cd [28].

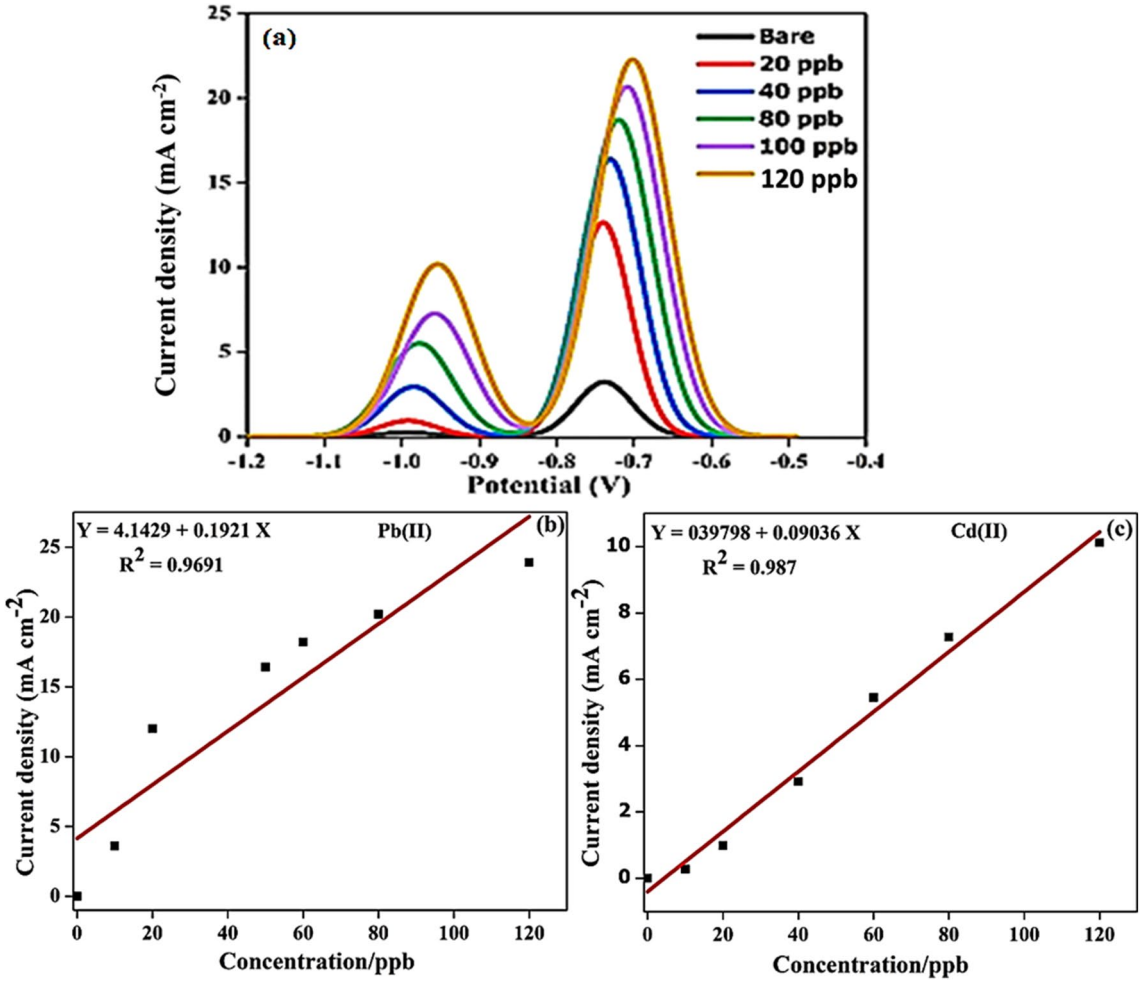

Fig. 9 Overlaid stripping voltammograms of the modified electrode in presence of different concentrations of Pb(II) and Cd(II) after a deposition time of 120 s at − 0.5 V and their corresponding calibration graphs

Table 1 Comparison of the analytical parameters of Co_3O_4 NPs@graphitic carbon /SPE in the determination of Pb(II) and Cd(II) with other existing sensors

Electrode	Technique	Linear range (ppb)		Limit of detection (ppb)		References
		Pb(II)	Cd(II)	Pb(II)	Cd(II)	
Sb NPs/BDDE	LSASV	50–500	50–500	24.4	38.1	[29]
Polyaniline/GCE	SWASV	0–414	0–224	20.7	14.56	[30]
NG/GCE	DPASV	10–900	100–900	50	5	[31]
MIL-100(Cr)/GCE	SWASV	100–1000	100–1000	48	44	[32]
HAP-nafion/GCE	DPASV	100–1000	100–1000	49	35	[33]
Alk-Ti_3C_2/GCE	SWASV	100–1500	100–1500	41	98	[34]
Calixarene functionalized Mn_3O_4/GCE	DPASV	100–1000	100–1000	7	9	[27]
Co_3O_4/SPE	DPASV	0–140	0–140	3.2	3.5	Present work

Sb NPs/BDDE antimony nanoparticles boron doped diamond; *Polyaniline/GCE* polyaniline modified glassy carbon electrode; *NG/GCE* N-doped graphene modified glassy carbon electrode; *MIL-100(Cr)/GCE* cauliflower-like *MIL-100(Cr)* modified glassy carbon electrode; Alk-Ti_3C_2/GCE *Alk-*Ti_3C_2 modified glassy carbon electrode; Co_3O_4*/GCE* cobalt oxide modified glassy carbon electrode

Table 2 Application study

Sample	Originally found (ppb)		Added (ppb)		Found (ppb)		Recovery (%)	
	Pb(II)	Cd(II)	Pb(II)	Cd(II)	Pb(II)	Cd(II)	Pb(II)	Cd(II)
Water Sample	22.5	ND	20	20	42.10	19.10	99.05	95.50

ND not detected, *ppb* parts per billion

3.12 Application study

To evaluate the proposed analytical method, the modified interface has been successfully applied for the quantification of Pb(II) and Cd(II) ions present in synthetically prepared water solution. 100 ppm of Pb(II) and Cd(II) standard solution was prepared in double distilled water and diluted to 1000 mL. Known volumes of the prepared standard Pb(II) and Cd(II) solution is added to the drinking water, supplied by Bangalore water supply and sewerage board, Bangalore, Karnataka, India. Finally, the stripping peak currents were measured, and the concentrations were correlated through the standard calibration plots. The observed results were compiled in Table 2.

4 Conclusions

The present work demonstrates the synthesis of uniformly distributed Co_3O_4 NPs@graphitic carbon by a simple and generic citrate–nitrate thermal decomposition method wherein the whole synthesis protocol completes within a few minutes (four minutes). The as-prepared uniformly distributed Co_3O_4 NPs@graphitic carbon were used as modifier for the modification of SPE to realize its potential applications in the quantification of toxic heavy metal ions Pb(II) and Cd(II) ions, present in aqueous solution. The proposed Co_3O_4 NPs@graphitic carbon/SPE demonstrate better sensing performance in terms of detection limit, which falls well below the threshold limit prescribed by WHO.

Acknowledgements The author, Ashoka S (SA) expresses sincere thanks to the Vision Group of Science and Technology (GRD-743/2017-18), Government of Karnataka for financial support.

Declarations

Conflict of interest There is no conflict of interest to declare.

References

1. Abu-Hayyeh S, Sian M, Jones KG, Manuel A, Powell JT (2001) Cadmium accumulation in aortas of smokers. Arterioscler Thromb Vasc Biol 21(5):863–867
2. Gao F, Gao C, He S, Wang Q, Wu A (2016) Label-free electrochemical lead (II) aptasensor using thionine as the signaling molecule and graphene as signal-enhancing platform. Biosens Bioelectron 81:15–22
3. Ndlovu T, Arotiba OA, Sampath S, Krause RW, Mamba BB (2011) Electrochemical detection and removal of lead in water using poly (propylene imine) modified re-compressed exfoliated graphite electrodes. J Appl Electrochem 41(12):1389–1396
4. Švancara I, Vytřas K, Barek J, Zima J (2001) Carbon paste electrodes in modern electroanalysis. Crit Rev Anal Chem 31(4):311–345
5. Van der Linden WE, Dieker JW (1980) Glassy carbon as electrode material in electro- analytical chemistry. Anal Chim Acta 119(1):1–24. https://doi.org/10.1016/S0003-2670(00)00025-8
6. Desimoni E, Brunetti B (2012) Glassy carbon electrodes film-modified with acidic functionalities. A review. Electroanalysis 24(7):1481–1500. https://doi.org/10.1002/elan.201200125
7. Yao Y, Wu H, Ping J (2019) Simultaneous determination of Cd (II) and Pb (II) ions in honey and milk samples using a single-walled carbon nanohorns modified screen-printed electrochemical sensor. Food Chem 274:8–15
8. Hong Y, Wu M, Chen G, Dai Z, Zhang Y, Chen G, Dong X (2016) 3D printed microfluidic device with microporous Mn_2O_3-modified screen printed electrode for real-time determination of heavy metal ions. ACS Appl Mater Interfaces 8(48):32940–32947
9. Niu P, Fernández-Sánchez C, Gich M, Navarro-Hernández C, Fanjul-Bolado P, Roig A (2016) Screen-printed electrodes made of a bismuth nanoparticle porous carbon nanocomposite applied to the determination of heavy metal ions. Microchim Acta 183(2):617–623
10. Oularbi L, Turmine M, Salih FE, El Rhazi M (2020) Ionic liquid/carbon nanofibers/bismuth particles novel hybrid nanocomposite for voltammetric sensing of heavy metals. J Environ Chem Eng 8(3):103774
11. Xin X, Hu N, Ma Y, Wang Y, Hou L, Zhang H, Han Z (2020) Polyoxometalate-based crystalline materials as a highly sensitive electrochemical sensor for detecting trace Cr (VI). Dalton Trans 49(14):4570–4577
12. Khalilzadeh MA, Tajik S, Beitollahi H, Venditti RA (2020) Green synthesis of magnetic nanocomposite with iron oxide deposited on cellulose nanocrystals with copper (Fe_3O_4@ CNC/Cu): investigation of catalytic activity for the development of a venlafaxine electrochemical sensor. Ind Eng Chem Res 59(10):4219–4228

13. Shreenivasa L, Prashanth S, Eranjaneya H, Viswanatha R, Yogesh K, Nagaraju G, Ashoka S (2019) Engineering of highly conductive and mesoporous ZrV 2 O 7: a cathode material for lithium secondary batteries. J Solid State Electrochem 23(4):1201–1209
14. Kumar N, Chowdhury AH, Bahrami B, Khan MR, Qiao Q, Kumar M (2020) Origin of enhanced carrier mobility and electrical conductivity in seed-layer assisted sputtered grown Al doped ZnO thin films. Thin Solid Films. https://doi.org/10.1016/j.tsf.2020.137916
15. Mishra TP, Neto RRI, Speranza G, Quaranta A, Sglavo VM, Raj R, Guillon O, Bram M, Biesuz M (2020) Electronic conductivity in gadolinium doped ceria under direct current as a trigger for flash sintering. Scripta Mater 179:55–60
16. Srinivasa N, Shreenivasa L, Adarakatti PS, Crapnell RD, Rowley-Neale SJ, Siddaramanna A, Banks CE (2020) Functionalized Co_3O_4 graphitic nanoparticles: a high performance electrocatalyst for the oxygen evolution reaction. Int J Hydrogen Energy 45(56):31380–31388
17. Hoekstra J, Beale AM, Soulimani F, Versluijs-Helder M, Geus JW, Jenneskens LW (2015) Base metal catalyzed graphitization of cellulose: a combined Raman spectroscopy, temperature-dependent X-ray diffraction and high-resolution transmission electron microscopy study. J Phys Chem C 119(19):10653–10661
18. Adarakatti PS, Gangaiah VK, Banks CE, Siddaramanna A (2018) One-pot synthesis of Mn_3O_4/graphitic carbon nanoparticles for simultaneous nanomolar detection of Pb (II), Cd (II) and Hg (II). J Mater Sci 53(7):4961–4973
19. Escudero-García R, Espinoza-Estrada E, Tavera F (2013) Precipitation of lead species in a Pb–H_2O system. Res J Recent Sci 9(4):1–8
20. Nikolaychuk PA (2018) The revised potential–pH diagram for Pb–H_2O system. Ovidius Univ Ann Chem 29(2):55–67
21. Tomlinson W, Campbell S, Carr S (1985) Thermodynamics of the Cd/H_2O system at 318 and 358 K and the corrosion of Cd as a function of pH. J Mater Sci Lett 4(6):715–719
22. Slavec M, Hocevar SB, Baldrianova L, Tesarova E, Svancara I, Ogorevc B, Vytras K (2010) Antimony film microelectrode for anodic stripping measurement of cadmium (II), lead (II) and copper (II). Electroanalysis 22(14):1617–1622
23. Majidian M, Raoof JB, Hosseini SR, Ojani R, Barek J, Fischer J (2020) Novel type of carbon nanotube paste electrode modified by sb_2o_3 for square wave anodic stripping voltammetric determination of Cd^{2+} and Pb^{2+}. Electroanalysis 32(10):2260–2265
24. Wang J, Zhao X, Li J, Kuang X, Fan Y, Wei G, Su Z (2014) Electrostatic assembly of peptide nano II ber–biomimetic silver nanowires onto graphene for electrochemical sensors. ACS Macro Lett 3(6):529–533
25. Kim S, Zhao P, Aikawa S, Einarsson E, Chiashi S, Maruyama S (2015) Highly stable and tunable n-type graphene field-effect transistors with poly (vinyl alcohol) films. ACS Appl Mater Interfaces 7(18):9702–9708
26. Organization WH (2010) Hardness in drinking-water: background document for development of WHO guidelines for drinking-water quality. World Health Organization
27. Adarakatti PS, Siddaramanna A, Malingappa P (2019) Fabrication of a new calix [4] arene-functionalized Mn_3O_4 nanoparticle-based modified glassy carbon electrode as a fast responding sensor towards Pb^{2+} and Cd^{2+} ions. Anal Methods 11(6):813–820. https://doi.org/10.1039/C8AY02648C
28. Babyak C, Smart RB (2004) Electrochemical detection of trace concentrations of cadmium and lead with a boron-doped diamond electrode: effect of KCl and KNO_3 electrolytes, interferences and measurement in river water. Electroanalysis 16(3):175–182. https://doi.org/10.1002/elan.200302794
29. Toghill KE, Xiao L, Wildgoose GG, Compton RG (2009) Electroanalytical determination of cadmium (II) and lead (II) using an antimony nanoparticle modified boron-doped diamond electrode. Electroanalysis 21(10):1113–1118
30. Wang Z, Liu E, Zhao X (2011) Glassy carbon electrode modified by conductive polyaniline coating for determination of trace lead and cadmium ions in acetate buffer solution. Thin Solid Films 519(15):5285–5289
31. Xing H, Xu J, Zhu X, Duan X, Lu L, Wang W, Zhang Y, Yang T (2016) Highly sensitive simultaneous determination of cadmium (II), lead (II), copper (II), and mercury (II) ions on N-doped graphene modified electrode. J Electroanal Chem 760:52–58
32. Wang D, Ke Y, Guo D, Guo H, Chen J, Weng W (2015) Facile fabrication of cauliflower-like MIL-100 (Cr) and its simultaneous determination of Cd^{2+}, Pb^{2+}, Cu^{2+} and Hg^{2+} from aqueous solution. Sens Actuators B Chem 216:504–510
33. Gao F, Gao N, Nishitani A, Tanaka H (2016) Rod-like hydroxyapatite and Nafion nanocomposite as an electrochemical matrix for simultaneous and sensitive detection of Hg^{2+}, Cu^{2+}, Pb^{2+} and Cd^{2+}. J Electroanal Chem 775:212–218
34. Zhu X, Liu B, Hou H, Huang Z, Zeinu KM, Huang L, Yuan X, Guo D, Hu J, Yang J (2017) Alkaline intercalation of Ti3C2 MXene for simultaneous electrochemical detection of Cd (II), Pb (II), Cu (II) and Hg (II). Electrochim Acta 248:46–57